

Experimental and Numerical Investigation of the Dispersion of Microparticles Emitted by Machining Operation

F. Tafnout, E. Belut, B. Oesterlé and J.R. Fontaine

Abstract—As a part of the development of a numerical method of close capture exhausts systems for machining devices, a test rig recreating a situation similar to a grinding operation, but in a perfectly controlled environment, is used. The properties of the obtained spray of solid particles are initially characterized using particle tracking velocimetry (PTV), in order to obtain input and validation parameters for numerical simulations. The dispersion of a tracer gas (SF_6) emitted simultaneously with the particle jet is then studied experimentally, as the dispersion of such a gas is representative of that of finer particles, whose aerodynamic response time is negligible. Finally, complete modeling of the test rig is achieved to allow comparison with experimental results and thus to progress towards validation of the models used to describe a two-phase flow generated by machining operation.

Keywords—Pollutants, capture, tracer gas, SF_6 , PTV, numerical modeling.

I. INTRODUCTION

HAND held tools, widely used in industry, are among the most polluting sources of dust in workplaces. Operators are highly exposed to large amounts of inhalable dust, which often carry a health hazard. Repeated exposure to these pollutants may lead to serious professional diseases, for instance mucosa irritation, hypersensitivity, pulmonary fibrosis or even cancer of the nasal and sinus cavities in the case of wood dust. As capturing pollutants as close as possible to the source represents the best way of preventing exposure, the design of close capture devices based on ventilation is of particular importance. That is why the « Institut National de Recherche et de Sécurité » (INRS) attempts to develop a method for optimal design of such devices, based on numerical simulation of air and dust flows by means of CFD (Computational Fluid Dynamics).

To validate the numerical models, an experimental test rig recreating a pseudo-grinding operation, but in a perfectly controlled environment, is achieved. A two-phase flow is obtained by the interaction of a jet of spherical glass particles with the airflow induced by the rotation of a cylinder. The spray of solid particles recreating the aerodynamic effects of a real particulate pollutant is produced by continuous injection

F. Tafnout is with the LEMTA laboratory (Université de Lorraine – UHP, CNRS) and with the INRS (Institut National de Recherche et de Sécurité), 54500 Vandœuvre-lès-Nancy, France (e-mail: fatma.tafnout@inrs.fr).

E. Belut and J.R. Fontaine are with the INRS (Institut National de Recherche et de Sécurité), B.P. 27, 54501 Vandœuvre-lès-Nancy, France (e-mails: emmanuel.belut@inrs.fr, jeanraymond.fontaine@inrs.fr)

B. Oesterlé is with the LEMTA laboratory (Université de Lorraine – UHP, CNRS), ESSTIN, 54519 Vandœuvre-lès-Nancy, France (e-mail: benoit.oesterle@esstin.uhp-nancy.fr).

of glass beads, using an endless screw which pushes them into a nozzle towards the rotating cylinder surface which removes them by friction. To provide a reference case for the development of numerical simulations, it is necessary to characterize the boundary conditions which are to be used for CFD predictions of the two-phase flow in the test facility. First, measurements of the glass particle velocities in the jet are performed using the particle tracking velocimetry (PTV) technique. This technique provides the characteristics of the jet, mostly near its source. Then, to experimentally evaluate the ability of numerical models to describe the dispersion of very fine particles, which behave like a passive tracer because of their negligible aerodynamic response time, a tracer gas (sulfur hexafluoride SF_6) is simultaneously injected at the source of the jet of glass particles, and its concentration field is measured using a gas analyzer. After a brief description of the test rig and the experimental techniques, the paper goes on describing a first attempt of numerical modeling of the involved multiphase flow. Comparisons between measurements and numerical results are then presented.

II. DESCRIPTION OF THE TEST FACILITY

The test rig, which reproduces a machining operation, involves a calibrated particle jet with controlled flow rate, generated by a rotating rough cylinder against a nozzle continuously fed with solid particles. The tracer gas, representing the passive pollutant (very fine particles), can be emitted at the jet source through a capillary tube. The device is placed in a ventilated test section to allow gas tracing measurements, as shown in Fig. 1. The angular velocity of the cylinder (diameter 130.5 mm, length 150 mm) is controlled by a frequency variator and regularly checked by means of a tachometer. As shown in Fig. 2, the particle injection system consists of two endless screws: the first one drives the particles (spherical glass beads, density 2500 kg m^{-3}) from the tank to the base of the second screw, which pushes the particles into a nozzle to the cylinder surface where they are tangentially ejected by friction.

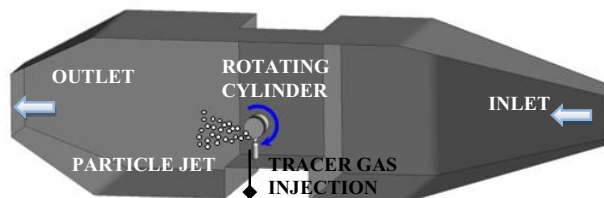


Fig. 1: Overview of the test rig

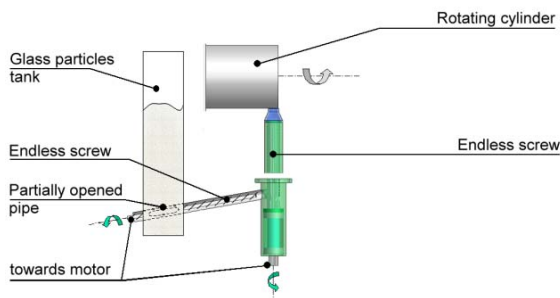


Fig. 2: Particle injection system

The particle size distribution has been characterized through a Malvern Mastersizer; the mean diameter of their equivalent Rosin-Rammler distribution is equal to $148 \mu\text{m}$ (Fig. 3). The emission rate is stable and pre-calibrated. In this study it is set to $1 \text{ g s}^{-1} \pm 6\%$, and two angular velocities of the cylinder are used: 500 rpm and 1000 rpm.

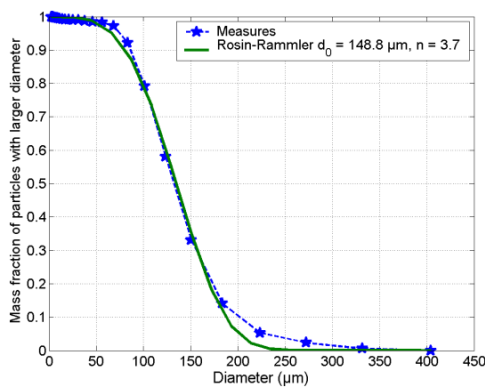


Fig. 3 Parameter estimation of the Rosin-Rammler law

III. MEASUREMENT OF PARTICLE VELOCITIES BY PTV

A. Measurement Tools

For the PTV measurements, a doubled laser Nd:YAG with two cavities is used, emitting pulses of wavelength 532 nm and energy 120 mJ. The CCD camera is a Hisense MkII (12 bits, 1344×1024 pixels). The assembly is mounted on a moving system and controlled by a computer using the Dynamic Studio Dantec software.

B. Development of the Particle Tracking Program

The general principle of the PTV method, similar to the particle image velocimetry (PIV), is divided as follows:

- 1) Illumination of a portion of the flow using a laser sheet, making the particles appear as bright spots ;
- 2) Acquisition of two successive images of the illuminated plane using a CCD camera ;
- 3) Image processing: measurement of individual particle velocity between two successive images.

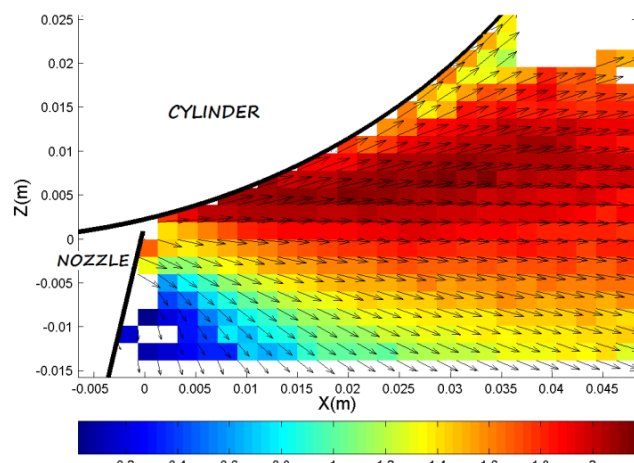
The principle is not to establish the mean motion of a set of particles as does the PIV, but rather to determine the displacement of single particles in successive images. The algorithm is divided into four main steps:

- 1) Equilibration of image background illumination by using the mean image of a sequence ;
- 2) Detection of particles on the image doublets ;
- 3) Particle pairing by determining the particle partners of the first image in the second one (pairing algorithm) ;
- 4) Calculation of particle motion between two images and validation. This step uses a subpixel interpolation [1] to estimate the exact displacement of the particles.

This algorithm, inspired by the method proposed by Vignal [2], has been the subject of extensive validation, through artificial translation of synthetic and real images, to assess its performances and to identify possible measurement errors. The test consists in imposing a uniform known translation to a given image, the translated image being calculated by cubic interpolation, and the PTV treatment is then applied between the original and translated images. Similarly, to approximate the experimental conditions, an additional test using the experimental translation of the image of a plate seeded with fixed particles has been achieved. These various tests have shown that the measurement error on the measured particle displacement is less than 3%.

C. Characterization of the Particle Jet Properties

The PTV program is used to measure the properties of the jet at its origin for various experimental parameters (angular velocity of the cylinder, mass flow rate of the jet). In Fig. 4, the mean particle velocities are displayed in the vertical plane of symmetry of the jet. In Fig. 5 the velocities are plotted in a YZ-section located at 8 mm from the source. An example of contour plot of the relative concentration of particles (normalized by the maximum value), estimated by computing the surface area of the detected particles, is shown in Fig. 6. For the results shown here, the angular velocity was 500 rpm and the jet mass flow rate was 1 g.s^{-1} .

Fig. 4: Mean axial velocity of particles in the XZ-plane (m.s^{-1})

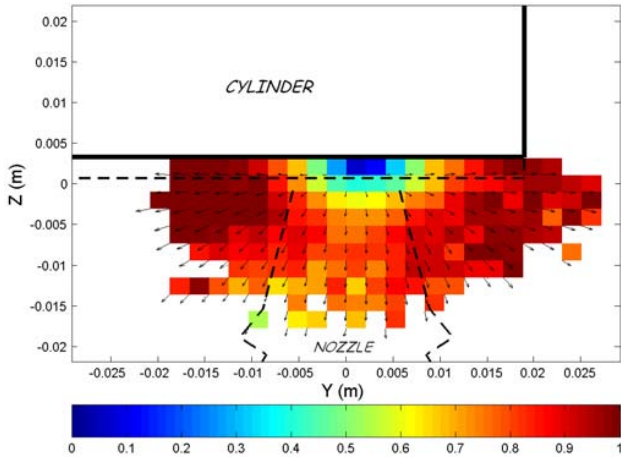


Fig. 5: Mean radial velocity of particles in a YZ-section located at 8 mm from the particle source ($\text{m}\cdot\text{s}^{-1}$)

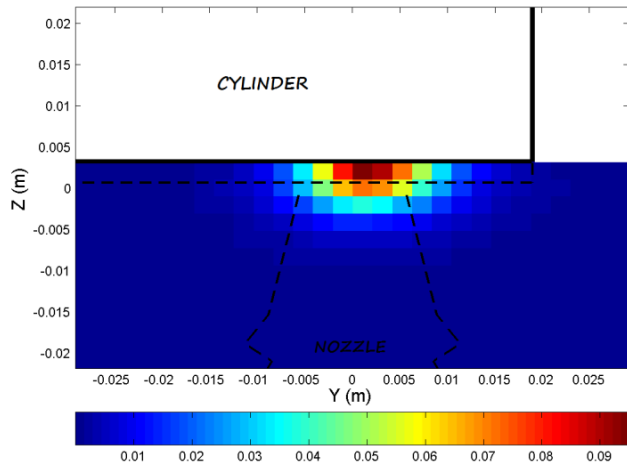


Fig. 6: Relative particle concentration in a YZ-section located at 8 mm from the particle source

IV. MEASUREMENT OF THE TRACER GAS CONCENTRATION

The dispersion of a tracer gas (sulfur hexafluoride, SF_6) emitted simultaneously with the particle jet has also been studied experimentally. Actually, such measurements are representative of the concentration of the finest machining particles, which have a very low aerodynamic response time. The experimental setup is designed to generate a tracer gas [3] at the source of the particle jet by means of a capillary tube, and then to measure the tracer gas concentration at several locations in the test section.

A. Description of the Experimental Setup

The experimental setup consists of two main parts:

- 1) An emission device of tracer gas (gas mixture SF_6/N_2 with 10% of SF_6 in volume) consisting of a flow regulator Bronkhorst EL-FLOW (capacity of $0\text{-}0.57 \text{ Nl min}^{-1}$ of mixture) and a capillary emission tube ;

- 2) Measurement and data acquisition system, consisting of 15 sampling probes (forming a rectangular grid of $50 \times 30 \text{ cm}$ of 5×3 sensors, spaced 10 cm from one another) connected to a gas analyzer (SF_6 , Wilks Infraran, cell 6.5 m, wavelength $10.68 \mu\text{m}$) and a computer with data acquisition program, allowing both acquisition and real-time monitoring of concentrations.

In addition to sampling probes inside the test section, the tracer gas concentration is measured continuously in the inlet section and at about 10 m from the outlet of the vein in the exhaust duct of diameter 200 mm. Monitoring the concentration in the vein inlet is used to evaluate the analyzer drift, while in the outlet it serves as a reference value for the concentration measurements, equal to the ratio of tracer and air flow rates in the vein owing to mixing.

To prepare the experimental campaign, a predictive numerical study of the test rig has been carried out beforehand, mainly to determine the air exchange rate in the tunnel and the tracer gas flow rate to be used in order to fulfill the following constraints:

- 1) Prevent the sensors from saturation, by avoiding concentrations above 7 ppm at the sampling points;
- 2) Convective effects due to the air flow rate should not prevail over the aerodynamic effects due to the particle jet and the cylinder rotation, which are the subject of this study.

This preliminary study led us to retain an air flow in the vein of $150 \text{ m}^3 \text{ h}^{-1}$ and a flow rate of tracer gas mixture below 0.04 Nl min^{-1} . It also helped identify an area of interest for positioning the sampling probes, namely a rectangle parallel to the YZ plane, centered at $Y = -13 \text{ cm}$ and $Z = 0$, and whose position along the X axis (approximate axis of the jet) can be adjusted. Both locations $X = 25 \text{ cm}$ and $X = 50 \text{ cm}$ have been chosen for the present measurements. The chosen coordinate system and the whole set-up are shown in Fig. 7.

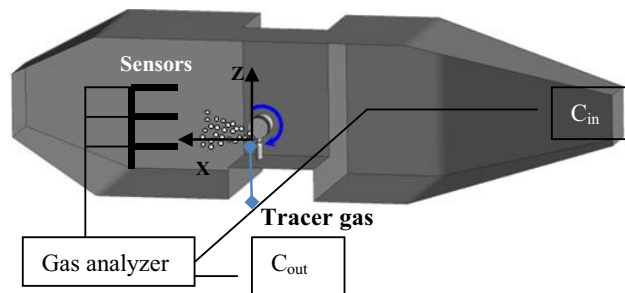


Fig. 7: Experimental set-up for tracer gas measurements

B. Measurement Protocol

The experimental protocol for the tests has been as follows:

- 1) Concentration measurement at the entrance of the vein, C_{in} , over a period of 100 s. This value allows evaluating the analyzer drift between the beginning and the end of a measurement cycle ;

- 2) Concentration measurement at one of the sampling point, C_{prel} , during 200 s ;
- 3) Concentration measurement at the end of the tunnel outlet pipe, C_{out} , during 200 s: reference concentration to normalize measurements and to allow proper comparison with numerical simulations ;
- 4) Control of the analyzer drift by new recording of concentration at the tunnel entrance C_{in} (100 s).

The acquisition times were chosen to achieve convergence of mean concentrations by at least 6% for each acquisition, with a 95% confidence interval. Every measurement was repeated four times for each probe location. The final results gather the four series of measurements with a final error taking into account the dispersion between each test and their own statistical uncertainties. An example of concentration record illustrating the measurement sequence is shown in Fig. 8.

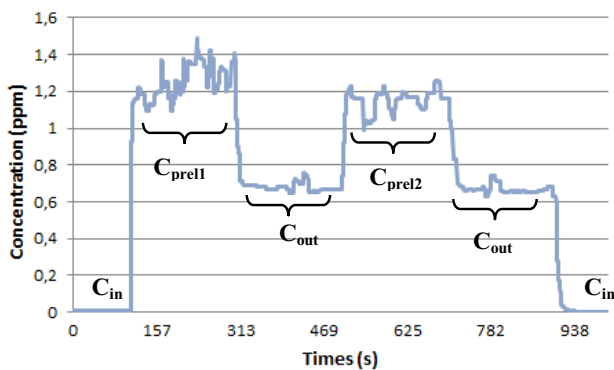


Fig. 8: Example of measurements : time evolution of concentration at 25 cm from the source (500 rpm)

C. Results of the Tracer Gas Measurement Campaign

The mean concentrations of SF_6 are normalized by the concentration of the outlet, after subtracting the concentration at the entrance of the tunnel in order to limit the errors due to possible analyzer drift. Thereby, we introduce the concentration ratio R , defined by the equation:

$$R = \frac{C_{prel} - C_{in}}{C_{out} - C_{in}} \quad (1)$$

The repeatability of concentration measurements has been verified, as well as the reproducibility of results on different days during which the experimental conditions were slightly varied (ambient temperature, atmospheric pressure, analyzer drift, small corrections in sensor positions, etc.).

The mean values of R shown later (Figs. 10, 12, 14) include error bars resulting from the repeatability of measurements during a single test, on the basis of a 95% confidence interval, as well as from the dispersion of results across trials.

V. NUMERICAL SIMULATION

Application of Computational Fluid Dynamics (CFD) to machining induced two-phase flows is still requiring developments, especially as regards proper prediction of the turbulence induced by the particle jet, and the subsequent accuracy of the prediction of the tracer gas dispersion (representative of ultra fine particles, whose aerodynamic response time is negligible). Providing measurements of tracer gas concentration in the tunnel will help validating the numerical modeling of machining induced two-phase flow. Thus, the purpose of this study is to evaluate the numerical models of transport of tracer gas inside the tunnel.

A. Numerical Approach

Gas phase: The studied airflow can be considered isothermal and incompressible. The *Realizable $k-\epsilon$* model, well described by Shih [4], is used to compute the mean flow and its turbulence properties, as a first attempt to simulate the flow. Standard wall functions are used for the wall boundary conditions.

Discrete phase: The glass particles emitted at the cylinder wall, recreating the effect of a real machining pollutant, are modeled using Lagrangian tracking. Particles input properties are deduced from the above described PTV measurements, by random drawing of initial particle size, location and velocity respecting the measurements made on the cross section of the jet at 8 mm from its source (including the overall mass flow rate and spatial distribution of the mass flow). The properties of the jet at 8 mm from the source are considered as representative of the emission conditions of particles. Given their initial velocity, the particles cross a distance of 8 mm in less than one tenth of their relaxation time. Their trajectories are integrated from the equation of motion for spherical particles, taking only into account the drag force and gravity. All other effects (added mass force, Basset...) are negligible in the present conditions. The instantaneous velocity of the fluid at the particle location being unknown (due to the choice of a RANS approach), a dispersion model is used to take into account the effect of turbulence on particle dispersion. The employed dispersion model is the Discrete Random Walk model (DRW) initially proposed by Hutchinson [5] and then developed by Gosman and Ioannides [6]. Proper choice of the particle time step was carried out according to Desjonqueres [7]. Particle collisions are not taken into account in this work, despite their possible influence close to the jet source region. The parcel method is used to describe particles: each computational particle represents a group of real particles of the same diameter. A single trajectory is calculated for each parcel, thus helping limit the number of computed trajectories. By considering, in the coupling terms, the real number of particles present in the parcel, the effect of the particles upon the airflow is properly taken into account. In the present case, one parcel contains four particles, and 316 000 trajectories are computed in the simulations.

Coupling Between the two phases: Backward momentum

coupling from particles to the mean flow is classically taken into account by considering the loss of momentum of all particles crossing each computational cell. Additional source terms are also considered in the $k-\epsilon$ equations to take into account the effects of particles on turbulence [8]-[9].

Tracer gas modeling: The SF₆ used experimentally is sufficiently dilute so that its effect on the flow is negligible. The transport equation for the SF₆ is therefore reduced to a simple convection-diffusion equation based on the mean flow of the fluid; turbulence increases locally the SF₆ diffusivity through a turbulent Schmidt number. In the simulations, the SF₆ concentration is normalized by the concentration at the exit of the tunnel (C_{out}), leading to the following transport equation for the ratio R :

$$\nabla R \cdot \mathbf{U} = \nabla \cdot \left\{ \left(D + \frac{\mu_t}{\rho S_{ct}} \right) \nabla R \right\} + S \quad (2)$$

where D denotes the molecular diffusivity of SF₆ in air, \mathbf{U} is the mean fluid velocity, μ_t is the turbulent viscosity, S_{ct} is the turbulent Schmidt number (assumed equal to 0.7) and S corresponds to the source of tracer gas at the jet source. Given the definition of R , this source term S is merely equal to the volume flow rate of air in the tunnel, owing to perfect mixing of SF₆ at the end of the tunnel exhaust pipe.

B. Results

In this section, numerical predictions of the ratio R are presented together with the corresponding experimental measurements. Concentration maps are provided in Figs. 9, 11, 13 and 15 for both angular velocities 500 and 1000 rpm, and for the two planes $X=25$ cm and $X=50$ cm. For further comparison, Figs. 10, 12, 14 and 16 display the evolution of the ratio R as a function of the Y location for the three values of Z considered in experiments. Lines are for the simulations, while symbols refer to the measurements.

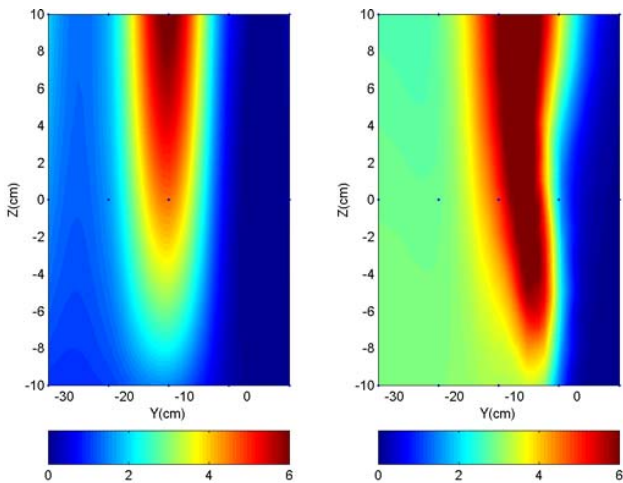


Fig. 9: Mean concentration maps, represented by the ratio R . Experimental (left) and numerical (right) results (500 rpm, $X=25$ cm)

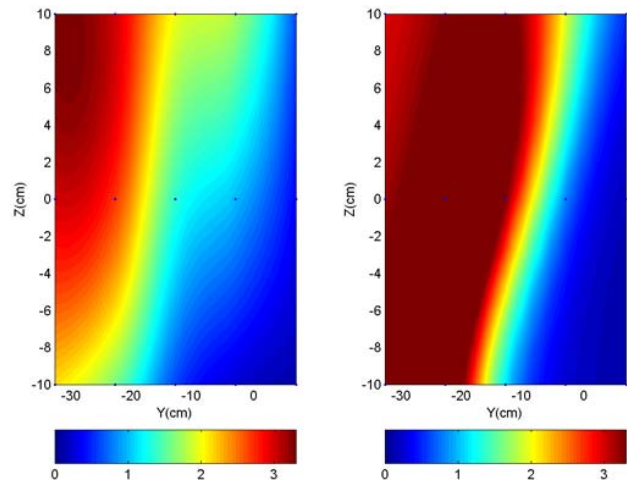


Fig. 11: Mean concentration maps, represented by the ratio R . Experimental (left) and numerical (right) results (500 rpm, $X=50$ cm)

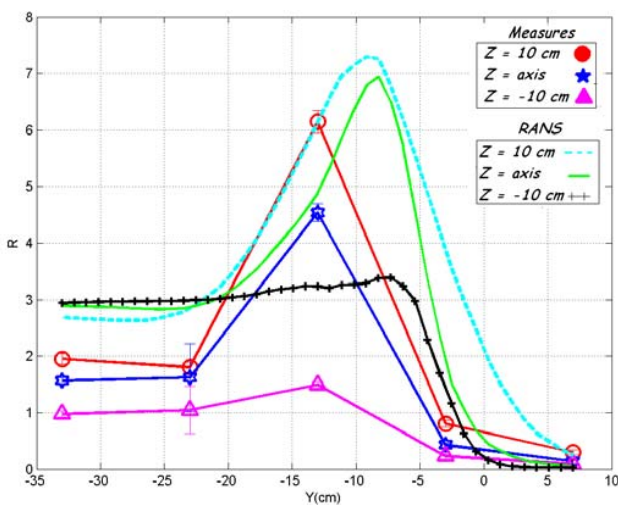


Fig. 10: Concentration profiles along the Y -axis (500 rpm, $X=25$ cm)

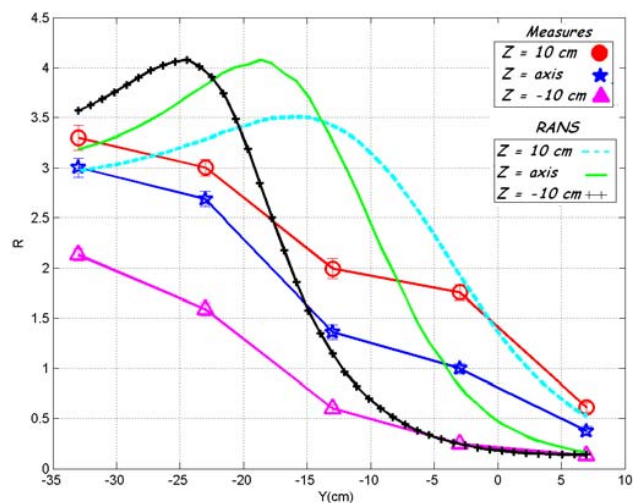


Fig. 12: Concentration profiles along the Y -axis (500 rpm, $X=50$ cm)

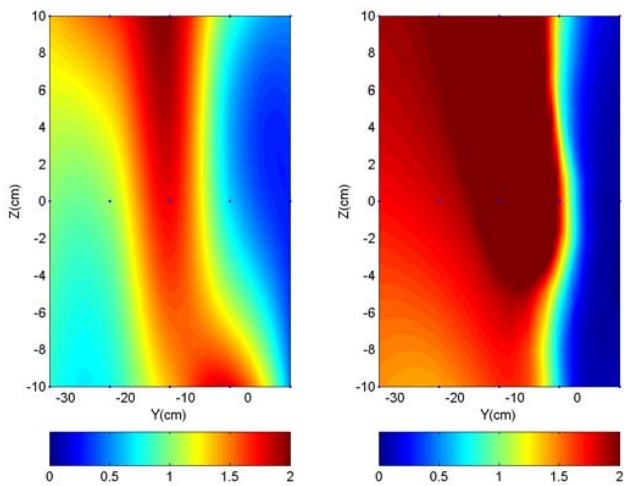


Fig. 13: Mean concentration maps, represented by the ratio R . Experimental (left) and numerical (right) results (1000 rpm, $X=25\text{cm}$)

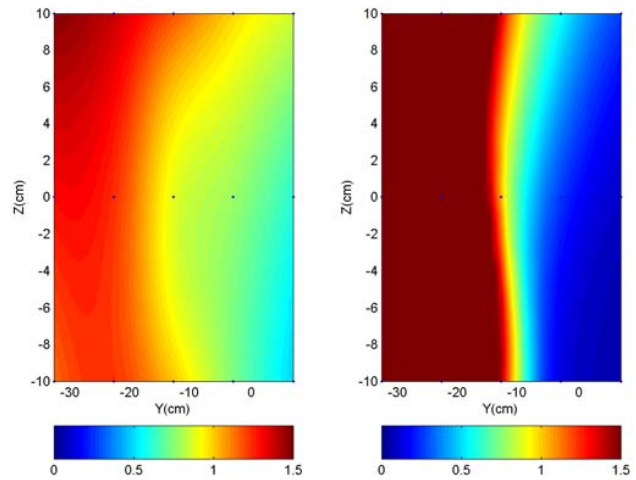


Fig. 15: Mean concentration maps, represented by the ratio R . Experimental (left) and numerical (right) results (1000 rpm, $X=50\text{cm}$)

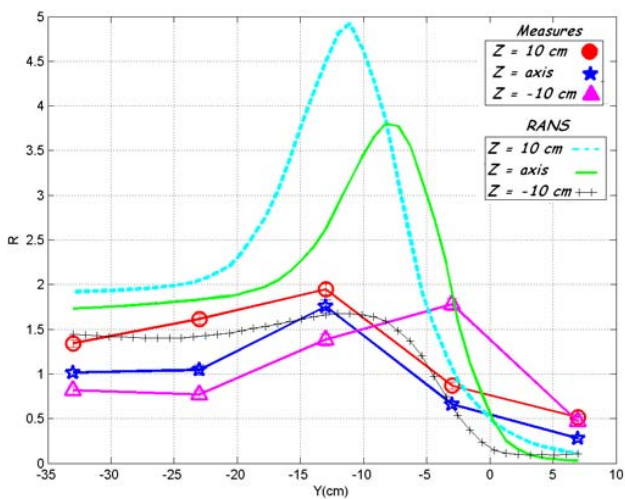


Fig. 14: Concentration profiles along the Y -axis (1000 rpm, $X=25\text{cm}$)

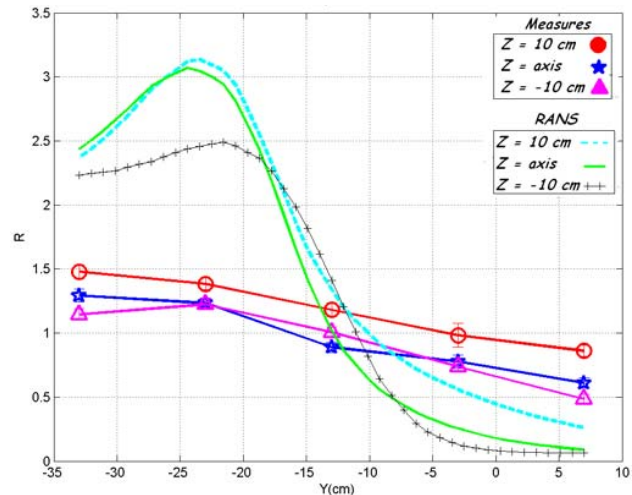


Fig. 16: Concentration profiles along the Y -axis (1000 rpm, $X=50\text{cm}$)

VI. DISCUSSION

The studied flow is representative, in its complexity, of machining induced two phase-flows, being controlled simultaneously by a rotating body and by a highly inertial jet of pollutant particles. As could be expected, RANS turbulence models perform correctly in predicting the dispersion of tracer gas despite some slight discrepancies. The observed dissimilarity between the measured and predicted tracer gas dispersion can be attributed to the modeling approach. Moreover, the measurement uncertainties in the tracer gas concentration are non negligible due to the intrusive feature of the experimental device.

As the area of contamination can be observed to extend beyond the measurement grid, the shape of the measured concentration profiles seems to partially challenge our choice of the sampling locations, thus confirming the objective we assigned to the numerical simulation.

It would be interesting to observe how some approach based on higher degree of modeling, like LES (large eddy simulation) or DES (detached eddy simulation) could provide more satisfactory results, as could be expected since no dispersion model is needed for the discrete phase in such approaches.

VII. CONCLUSION

With the objectives of developing a method for optimal design of capture devices for pollutant particles emitted by machining operations, both experimental and numerical investigations have been carried out. An experimental test rig recreating a pseudo-grinding operation has been built in order to assess the capabilities of various numerical models. Velocity profiles of a solid particle flow induced by friction against a rotating cylinder (simulating the emission of a real particulate pollutant) have been measured using the PTV technique (particle tracking velocimetry). The diffusion of the population of finest particles, which behave like tracers, has been characterized by measurements of the concentration field of a tracer gas emitted simultaneously with the particle jet.

Future work will be dedicated to evaluation of the so called detached eddy simulation approach (DES) when applied to the present case. Additional measurements concerning the velocity fields of air and particles are planned to complement the experimental data.

REFERENCES

- [1] M. Marxen, P. E. Sullivan, M. R. Loewen and B. Jaohne, "Comparison of Gaussian particle center estimators and the achievable measurement density for particle tracking velocimetry," *Exp. Fluids*, vol. 29, pp. 145-153, 2000.
- [2] L. Vignal, *Chute d'un nuage de particules dans une turbulence diffusive. Etude du couplage entre phases par diagnostics optiques*, PhD thesis, Institut National Polytechnique de Toulouse, France, 2006.
- [3] R. Niemelä, *Characterization of the performance of industrial ventilation systems by the tracer gas technique*, Institute of Occupational Health, Helsinki, Finland, ISBN 951-801-556-2, 1986.
- [4] T. Shih, W. Liou, A. Shabbir and J. Zhun, "A new $k-\epsilon$ eddy-viscosity model for high Reynolds number turbulent flows - Model development and validation," *Computers in Fluids*, vol.24, pp. 227-238, 1995.
- [5] P. Hutchinson, G. F. Hewitt and A. E. Dukler, "Deposition of liquid or solid dispersions from turbulent gas stream : a stochastic model," *Chem. Engng. Sci.*, Volume 26, pp 419-439, 1971.
- [6] A. D. Gosman, E. Ioannides, "Aspects of computer simulation of liquid-fuelled combustors," *J. Energy*, vol.7, pp.482-490, 1983.
- [7] P. Desjonquères, *Modélisation lagrangienne du comportement de particules discrètes en écoulement turbulent*, PhD thesis, Université de Rouen, France, 1987.
- [8] A. A. Amsden, P. J. O'Rourke and T. D. Butler. *KIVA-2 : a computer program for chemically reactive flows with sprays*, Technical Report LA-11560-MS, UC-96, Los Alamos National Laboratory, Los Alamos, New Mexico, May 1989.
- [9] G. M. Faeth. "Spray atomization and combustion," *AIAA-1986-0136*, 24th Aerospace Sciences Meeting, Reno, NV, USA, 1986.